Chinese Chemical Letters 32 (2021) 2856–2860

Contents lists available at ScienceDirect

Chinese Chemical Letters

journal homepage: www.elsevier.com/locate/cclet

Communication

A novel phosphorus oxide quantum dots as an emissive nanomaterial for inorganic ions screening and bioimaging

Zhen Fang, Yuting Liang, Xiaomei Wang, Shuhan Zhang, Jun Yu, Hu Xu*, Yuhong Wang*

Research Institute of Applied Catalysis, School of Chemical and Environmental Engineering, Shanghai Institute of Technology, Shanghai 201418, China

ARTICLE INFO

Article history:
Received 6 November 2020
Received in revised form 10 January 2021
Accepted 9 February 2021
Available online 15 February 2021

Keywords:
Phosphorus oxide quantum dots
Emissive material
Bioimaging
Ion screening
Iodine ion
Iron ion

ABSTRACT

In this work, a novel blue-green fluorescence phosphorous oxide quantum dots (PO QDs) was synthesized by solvothermal method in *N*-methyl-2-pyrrolidone (NMP) solution without any protection treatment during synthesis. Upon excitation at 400 nm, PO QDs emitted blue-green fluorescence with quantum yield of 0.28. PO QDs exhibited the high inertness to air or moisture, the excellent water solubility, and stable emission intensity in a wide pH range and in high ionic strength solution. Interestingly, PO QDs could give the positive optical response to iron ions (Fe^{3+}) and iodine ion (I^-). The photoluminescence (PL) of PO QDs could be directly quenched by Fe^{3+}. While I^- quenched the PO QDs PL by means of Ag^+-mediated PO QDs system *via* the internal filtration effects (IFE) induced by the formation of AgI. Moreover, the biocompatibility and low toxicity of PO QDs verified in bean sprout and Hela cells indicated the promising application of PO QDs in medicine related fields. Furthermore, PO QDs could also be utilized in luminescent composite film for various application scenarios

Black phosphorus (BP) as a novel nanomaterial has aroused enormous interest in the fields of electro-photocatalysis, energy storage, photo-transistor, medical therapy related application due to the distinctive features such as layer-dependent bandgap (0.3–2.0 eV), large extinction coefficient in near infrared region (14.8 L g^{-1} cm^{-1} at 808 nm), high charge carrier mobility, long exciton lifetime, high photothermal conversion efficiency, and facile surface modification [1–5]. BP-based nanomaterial has been used as optical sensors for explosive [6,7], gas [8,9], pH [10,11], biothiols [12], biomolecules [13–17], and acetylcholinesterase activity [18]. To date, more BP nanomaterials as fluorescent probes focused on biomolecules [13–17]. However, the studies for inorganic ions by fluorescent BP nanomaterials are really rare. Gu *et al.* reported a BP quantum dots (BP QDs) based ratiometric fluorescence sensor for Hg^{2+} [19]. Tetraphenylporphyrin tetrasulfonic acid (TPPS) could quench the fluorescence of BP QDs by the inner filter effect (IFE). The presence of Hg^{2+} accelerated the complex between Mn^{2+} and TPPS, which weaken the IFE between TPPS and BP QDs. Thus, the fluorescence of BP QDs (green color) and TPPS (red color) was recovered and decreased, respectively. Yue *et al.* reported a fluorescence turn-on probe for pH (H^+) by using a green-emitted BP QDs *via* the protonation and deprotonation of BP QDs surface [10]. More recently, a fluorescence method for the detection of Hg^{2+} and Cu^{2+} by BP QDs was also reported, in which the fluorescence of BP QDs could be directly quenched by these two metal ions [20]. However, BP-based materials are extremely sensitive to circumstance air or moisture [21]. The tedious synthesis and purification process of BP without oxygen and moisture considerably limits the fast and on-site application. As for the solvothermal synthesis of BP nanomaterial, the presence of high boiling point solvent such as *N*-methyl-2-pyrrolidinone (NMP) in product is always an obstacle for the practical application because of its difficult separation from BP QDs [13]. Furthermore, there is not a report focusing on anion detection by fluorescent BP based nanomaterials. Thus, the development of phosphorus containing nanomaterial with high inertness to air or moisture, excellent stability, facile synthesis, and high luminescence efficiency is really desired.

Herein, we reported the synthesis and fluorescence application of a novel phosphorus containing nanoparticle *i.e.*, phosphorus oxide quantum dots (PO QDs) as emissive material. PO QDs with blue-green emission were obtained from the common solvothermal method by using phosphorus pentaoxide (P_2O_5) as starting material and purified by column chromatography. The resulting emissive PO QDs exhibited the excellent water solubility and stable emission feature in a wide pH range and in high ionic strength solution. Interestingly, PO QDs could response positively to iron

* Corresponding authors.
E-mail addresses: xuhu@sit.edu.cn (H. Xu), yuhong_wang502@sit.edu.cn (Y. Wang).

https://doi.org/10.1016/j.cclet.2021.02.024
1001-8417/

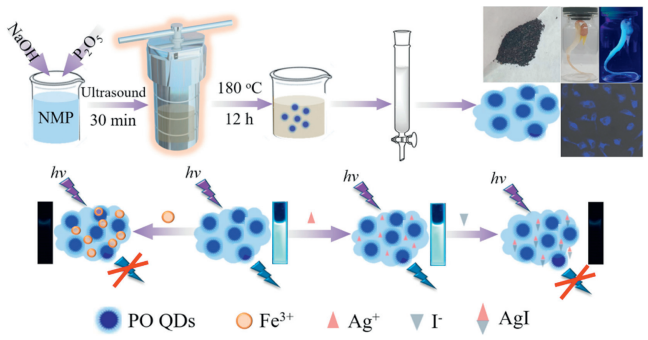

Scheme 1. Schematic illustration of the synthesis, physical photographs, fluorescence screening Fe^{3+} and I^-, and bioimaging applications of PO QDs in live bean sprout and Hela cells.

ions (Fe^{3+}) and iodine ion (I^-) in different response modes (Scheme 1). The photoluminescence (PL) of PO QDs could be directly quenched by Fe^{3+}. While the detection of I^- was realized by means of Ag^+-mediated PO QDs system *via* PL quenching. More importantly, the low toxicity of PO QDs demonstrated in bean sprout indicated that this novel PO QDs nanomaterial could be utilized in bioimaging or medicinal diagnostics. Furthermore, PO QDs could also be utilized in luminescent composite film for various promising applications.

Emissive PO QDs were synthesized from P_2O_5 as the precursor *via* solvothermal method without any protection measures used in BP synthesis. Typically, P_2O_5 (500 mg) was dispersed in NaOH (500 mg)/NMP (150 mL) solution and sonicated for 0.5 h. Then the solution was stirred vigorously for 12 h at 180 °C. The presence of NaOH facilitated the formation and stability of PO QDs [22]. During this process, the color of the solution gradually changed from colorless to deep yellow. The crude product was purified by silica column chromatography by using petroleum ether/ethyl acetate (volume ratio from 3:1 to 1:1) as the eluent. The resulted black solid was dried at 120 °C. The product was re-dissolved in pure water (0.01 mg/mL) as PO QDs stock solution for further use. The PL quantum yield (QY) of as-prepared PO QDs was determined by an indirect method using sodium fluorescein (0.95 in water [23]) as the standard reference (Supporting information). The PL QY of PO QDs was estimated to be 0.28.

X-ray photoelectron spectroscopy (XPS) and Fourier transform infrared spectroscopy (FTIR) spectroscopy were firstly performed for both the pristine P_2O_5 powder and PO QDs. The FTIR spectrum of PO QDs showed the strong peaks at 1661, 1260, and 1117 cm^{-1} (Fig. 1a). The peaks at 1661 and 1260 cm^{-1} were assigned to the P=O stretching and vibrational modes, respectively [24]. The peaks at 1117 cm^{-1} were assigned to the P—O stretching mode. Staring material P_2O_5 also showed a characteristic set of peaks at 1661, 1210, and 1006 cm^{-1} in its FTIR spectrum. The broad peak centered at 1006 cm^{-1} was ascribed to the P—O stretching mode. The presence of P=O and P—O bonds in PO QDs was also confirmed by subsequent XPS analysis. Fig. 1b showed the XPS full spectrum of PO QDs, which included two sets of peaks corresponding to O 1s and P 2p, respectively. This indirectly indicated the co-existence of O and P elements in the as-prepared PO QDs. The P 2p signal could be deconvoluted into two peaks at around 134.9 and 135.8 eV assigning to P—O and P=O bonds, respectively (Fig. 1c) [19]. Similarly, the high resolution O 1s spectrum (Fig. 1d) exhibited two peaks located at 531.7 and 533.2 eV that were associated with non-bridging oxygen (P=O) and singly bonded oxygen (P—O), respectively [25]. These results confirmed that PO QDs had been successfully synthesized. The structural characterization of PO QDs was further investigated by transmission electron microscopy (TEM). As shown in Fig. 1e, these nearly dot-like PO QDs with average diameter of 6.4 ± 1.2 nm were uniform and well-dispersed suggesting no evident aggregation. The clear lattice fringe with interplanar spacing of 0.231 nm shown in high-resolution transmission electron microscopy (HRTEM) indicated the good crystallinity of the as-prepared PO QDs (the inset in Fig. 1e). Compared with common BP QDs with particle size *ca.* 1.7 nm [18,19], our PO QDs in this study possess a relatively large size with an average

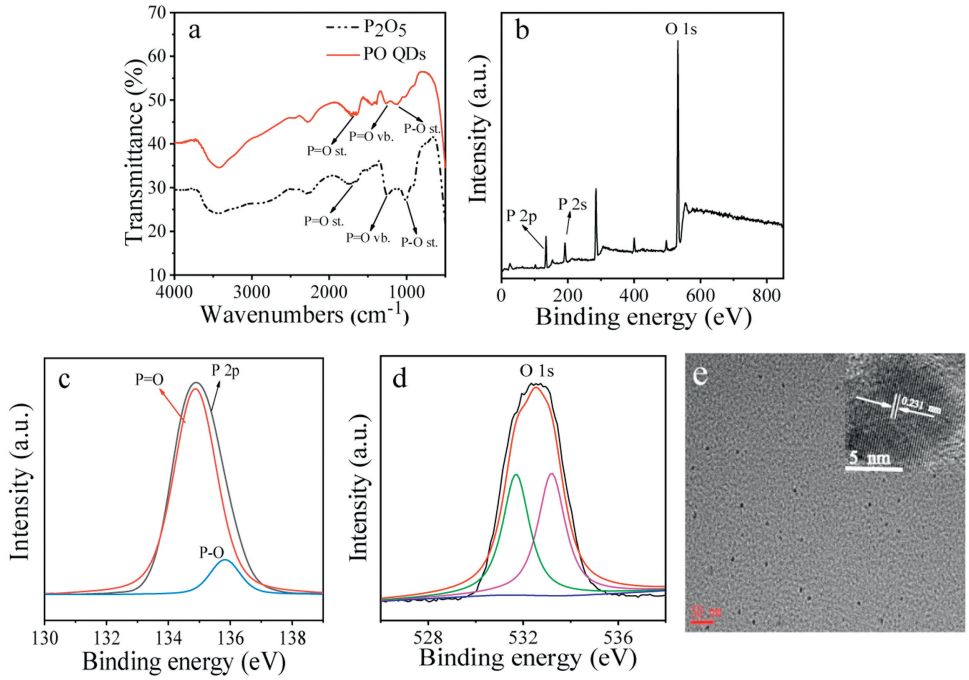

Fig. 1. (a) Solid-state FTIR spectra of PO QDs (red line) and P_2O_5 powder (black dash dot line). XPS full scan spectrum (b), high resolution XPS spectra of P 2p (c) and O 1s (d) of PO QDs. (e) Wide-field TEM image of PO QDs, the insert represents the corresponding HRTEM.

diameter of 6.4 ± 1.2 nm. Apart from the difference in QDs size, there is an evident difference in valence state of P element between BP QDs and PO QDs. In BP QDs, P element existed mainly at P◦ with partial oxidation of BP QDs [18,19], while only P^V was observed in our PO QDs implying the presence of P—O and P=O bonds (Fig. 1c). All these results suggested that PO QDs have been successfully synthesized.

UV–vis absorption, excitation, and PL spectra were also used to investigate the fundamental optical properties of PO QDs (Fig. S1 in Supporting information). Like BP QDs, PO QDs synthesized *via* solvothermal method emitted a blue-green fluorescence under UV light (the inset in Fig. S1a). Fig. S1b reveals the excitation-dependent PL of PO QDs, and the emission peak can be red-shifted from 450 nm to 545 nm by varying excitation wavelength. And the maximum emission peak appeared at 490 nm upon excitation at 400 nm, which may attribute to the polydispersity of QDs. Meanwhile, the stability of PO QDs was also evaluated in phosphate buffer saline (PBS) buffers with different pH values and NaCl solutions with different concentrations. As shown in Fig. S2a (Supporting information), the PL intensity of PO QDs was relatively stable in the pH range below 7.5, which demonstrated that PO QDs could exist stably in acidic and near neutral condition. With the increase of solution pH into basic condition, the PL intensity of PO QDs would decreased quickly, which might be associated with the increase of the amount of QDs surface trap state. After all the high pH condition greatly promoted the de-protonation of −P(O)−OH on QDs surface and accumulated the negatively electric charge of QDs surface, which could induce the more channels for the non-radiative recombination. The relatively constant PL intensities of PO QDs in NaCl solutions with different concentrations (0–1.0 mol/L) demonstrated the excellent resistance of PO QDs against high ionic strength (Fig. S2b in Supporting information). In PBS solutions, PO QDs could be stored for 6 months without the evident change in PL intensity, which also suggested the high thermodynamic stability of PO QDs (Fig. S2c in Supporting information). XPS spectrum of PO QDs did not exhibit the evident change even exposure to air for 6 months in dark (Fig. S2d in Supporting information). These results implied the high stability of PO QDs to air or moisture.

Like other QDs, such as carbon dots (CDs) and graphene QDs, the PL of PO QDs can be greatly influenced by the interactions between QDs surface functional groups and foreign substances. Once this interaction occurs on the surface of QDs, the corresponding optical response will be observable. For instance, Wang *et al.* developed a polyethyleneimine functionalized CDs-based probe for Cu^{2+} in living cells *via* electron transfer process [26]. In our case, PO QDs was relatively inert towards Cu^{2+}, but was fairly sensitive to Fe^{3+} leading to PL quenching, which might be due to the charge transfer between Fe^{3+} and PO QDs. Due to the strong oxidation ability, Fe^{3+} confined on PO QDs surface readily captured the electrons from the lowest unoccupied molecular orbital (LUMO) of PO QDs upon excitation, which inhibits the re-transition of electrons from LUMO to the highest occupied molecular orbital (HOMO) of PO QDs resulting in the weak fluorescence (Fig. 2a, Figs. S3a and b in Supporting information). To gain the insight of PL quenching of PO QDs by Fe^{3+}, Stern-Volmer experiment was performed. As shown in Fig. 2b, a downward curve could be obtained, which indicated that higher Fe^{3+} content could quench effectively the PL of PO QDs. The PL intensity ratio F/F_0 exhibited two excellent linear relationship with Fe^{3+} concentration (one was the Fe^{3+} concentration range of 0.14−0.98 mmol/L with R^2 = 0.9939 and the other was Fe^{3+} concentration range of 0.98–1.82 mmol/L with R^2 = 0.9640). Moreover, PO QDs exhibited the fast PL response (the insert of Fig. 2b) and high selectivity to Fe^{3+} (Figs. S4a and S4b in Supporting information).

Unlike the response of PO QDs towards Fe^{3+}, no evident PL change of PO QDs was observed upon direct adding I^-. Considering the photosensitive characteristic of silver iodide (AgI) [27], we speculated that I^- could positively respond to Ag^+-mediated PO QDs. Fortunately, Ag^+ did not impose any effect on the PL of PO QDs, which enabled us to have chance to investigate the response of Ag^+-mediated PO QDs to I^-. Primary study supported our inference. The addition of I^- into Ag^+-mediated PO QDs could induce an evident PL quenching (Fig. 2c), which might be due to the formation of AgI and the subsequent internal filtration effects (IFE) between AgI and PO QDs (Figs. S3c, S5, and Table S1 in Supporting information). Stern-Volmer experiment verified the I^- content dependent PL quenching feature (Fig. 2d). The amount of Ag^+ in Ag^+-mediated PO QDs was an important factor to the sensitivity of this fluorescent probe. For five Ag^+ concentrations tested, 0.40 mmol/L of Ag^+ concentration gave the best optical response (Fig. S6a in Supporting information). Under the optimal condition, a linear relationship between F/F_0 and I^- concentration was found within I^- concentration range from 0.047 to 0.376 mmol/L (R^2 = 0.9669). The PL response of Ag^+-mediated PO QDs towards I^- was so fast that the PL of Ag^+-mediated PO QDs was almost immediately quenched by I^- within several seconds (the inset in Fig. 2d), which reflected the ultrafast reaction kinetic characteristic between them. The excellent selectivity of Ag^+-mediated PO QDs to I^- demonstrated the practicability as a fluorescent probe (Figs. S4c and d in Supporting information). In addition, the broad pH application condition enables PO QD-based fluorescent probes to fit various real scenes for Fe^{3+} and I^- (Fig. S6b in Supporting information). The comparison for Fe^{3+} detection (Table S2 in Supporting information) and I^- detection (Table S3 in Supporting information) between PO QDs and other nanomaterils/methods have been summarized in Supporting information, which

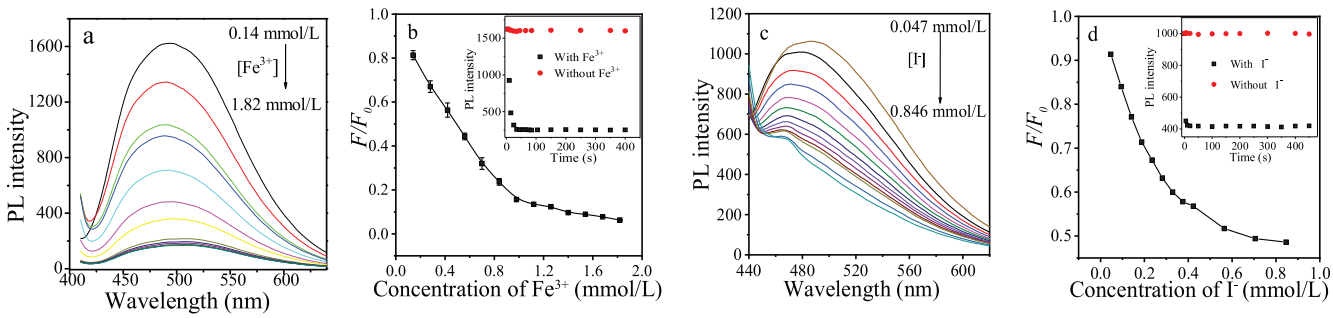

Fig. 2. (a) The PL spectra of PO QDs suspension *vs.* varying Fe^{3+} concentrations. (b) The relationship between F/F_0 and increasing Fe^{3+} concentration in (a) (the inset represents the PL response time of PO QDs suspension toward Fe^{3+} (1.2 mmol/L) at pH 6.0). (c) The corresponding PL spectra of Ag^+-mediated PO QDs suspension *vs.* varying I^- concentrations. (d) The relationship between F/F_0 and I^- concentration in the presence of increasing I^- content (the inset represents the PL response time of Ag^+-mediated PO QDs suspension toward I^- (0.8 mmol/L) at pH 6.0).

demonstrated the dual detection mode for different inorganic ions using the same PO QDs.

As an emissive nanomaterial, PO QDs used in bioimaging is a promising application scenarios. Thus, we attempted the fluorescence imaging of PO QDs in the living bean sprouts. The aqueous solution containing PO QDs was used to culture bean sprouts during the whole period of growth. As shown in Fig. 3a, PO QDs could be easily assimilated by the plant cells. Upon UV light illumination, the whole body of bean sprouts with PO QDs culturation exhibited the evident blue-green fluorescence compared to those without PO QDs culturation, which definitely demonstrated the excellent biocompatibility of PO QDs (Fig. S7 in Supporting information). Moreover, the visible fluorescence images of bean sprouts during the whole period of growth suggested the low toxicity of PO QDs, which was also a very important factor in bioimaging. As for all the test cases (200 cases), the germination rate of mung bean was 100% and there was no any case of abnormal death by PO QDs uptake. In addition to bean sprouts, we also investigated the cellular imaging of Hela cells by PO QDs (Fig. 3b). Without culturation of PO QDs, live Hela cells did not display any fluorescence response. After incubation with PO QDs (1×10^{-5}, 5×10^{-5} and 10×10^{-5} mg/mL) for 0.5 h respectively, all Hela cells showed the fluorescence "off-on" response implying the effective *in vitro* imaging feature of PO QDs. The concentration dependent characteristic was also relatively distinct. Compared to the fluorescence images with low concentration of PO QDs (1×10^{-5} and 5×10^{-5} mg/mL), Hela cells with higher PO QDs concentration (10×10^{-5} mg/mL) produced the stronger fluorescence. These results fully indicate that the as-prepared PO QDs possess the good biocompatibility and low toxicity, which enables it to be applied in bioimaging or biomedical diagnosis.

Luminescent composite film has been widely used in various fields including industrial production, military field, aerospace, crafts, fire safety *etc*. The excellent dispersion of PO QDs in hydrophilic and hydrophobic solvents including ethanol (EtOH), tetrahydrofuran (THF), dimethylformamide (DMF), dichloromethane (CH_2Cl_2), chloroform ($CHCl_3$), ethyl acetate (EA), and petroleum ether (PE) made it easy to prepare the luminescent composite film. Moreover, the difference of solvent polarity did not significantly affect the emissive property of PO QDs (Fig. S8a in Supporting information). By mixing PO QDs and polyvinyl alcohol (PVA) in water, a flexible transparent luminescent composite film PO QDs-PVA could be readily obtained after evaporating the solvent. The good dispersion in PVA matrix ensured the homogeneous blue-green fluorescence in solid film (Fig. S8b in Supporting information). The solidification of PO QDs in PVA film imposed little effect on the emissive property as shown by the distinct "**SIT**" signs. The resulted PO QDs-PVA composite film possessed the excellent photostability. There was no evident fluorescence change in PO QDs-PVA film even after exposure to sunlight for 30 days (Fig. S8b). The excellent stability of PO QDs in PVA film may be ascribed to the multisite interaction between PO QDs and hydroxyl groups in PVA. In addition to luminescent composite film, the emissive PO QDs could be sprayed to the surface of different substrates such as rubber mat, plastic plate, glass pane, paperboard, and iron plate. All the PO QDs coated materials emitted the blue-green fluorescence upon illumination of UV light (Fig. S8c in Supporting information).

We have developed a novel blue-green light emitted PO QDs with high PL QY of 0.28, excellent dispersion ability in hydrophilic and hydrophobic media and good photostability. PO QDs can be used as the promising probe for inorganic ions such as Fe^{3+} and I^- in aqueous media. Moreover, the new emissive PO QDs have successfully achieved the bioimaging in live bean sprouts and Hela cells together with serving as PO QDs-PVA nanocomposite film demonstrating the promising applications for various scenarios.

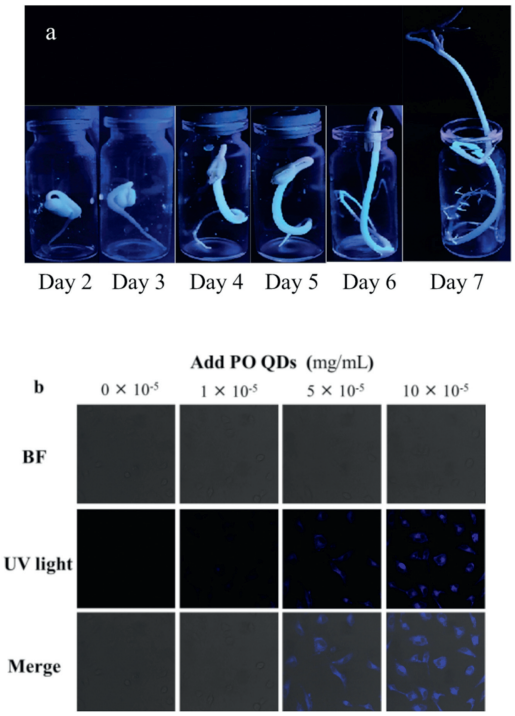

Fig. 3. (a) Fluorescence images of bean sprouts cultured by PO QDs during the period of growth. (b) Fluorescence microscopic images under bright field (BF), UV light, and merged images of Hela cells incubated with PO QDs (1×10^{-5}, 5×10^{-5}, and 10×10^{-5} mg/mL) for 0.5 h.

Declaration of competing interest

The authors declare that they have no known competing financial interests or personal relationships that could have appeared to influence the work reported in this paper.

Acknowledgment

We thank the National Natural Science Foundation of China (No. 21808142) for financial support.

Appendix A. Supplementary data

Supplementary material related to this article can be found, in the online version, at doi:https://doi.org/10.1016/j.cclet.2021.02.024.

References

[1] Z. Sun, H. Xie, S. Tang, et al., Angew. Chem. Int. Ed. 54 (2015) 11526–11530.
[2] H. Wang, X. Yang, W. Shao, et al., J. Am. Chem. Soc. 137 (2015) 11376–11382.
[3] D.P. Dubal, N.R. Chodankar, D.H. Kim, P.T. Gomez-Romero, Chem. Soc. Rev. 47 (2018) 2065–2129.
[4] A. Hirsch, F. Hauke, Angew Chem. Int. Ed. 57 (2018) 4338–4354.
[5] J.H. Ryu, H.J. Kim, K. Kim, et al., Adv. Funct. Mater. 29 (2019) 1900495.
[6] L. Houjing, S. Mingxia, S. Yingying, et al., Chem. Commun. 54 (2018) 7987–7990.
[7] R.L. Kumawat, B. Pathak, Appl. Surf. Sci. 529 (2020) 147094.
[8] H. Ren, Y. Zhou, Y. Wang, et al., Sens. Actuators B: Chem. 321 (2020) 128520.
[9] K. Rathi, K. Pal, ACS Appl. Mater. Interfaces 12 (2020) 38365–38375.
[10] Q. Yue, Y. Hu, L. Tao, et al., Mikrochim. Acta 186 (2019) 640.
[11] P. Guo, W.H. Song, S. Yan, Opt. Commun. 406 (2018) 91–94.
[12] L. Ren, H. Li, J. Du, Microchim. Acta 187 (2020) 229–236.
[13] I.E.V. Rosales, L. Rovigatti, E. Bianchi, C.N. Likos, E. Locatelli, Nanoscale 12 (2020) 21188–21197.
[14] Y.T. Yew, Z. Sofer, C.C. Mayorga-Martineza, M. Pumera, Mater. Chem. Front. 1 (2017) 1130–1136.

[15] J. Zhou, Z. Li, M. Ying, et al., Nanoscale 10 (2018) 5060–5064.
[16] Z. Hua, Y. Lia, E. Hussaina, et al., Talanta 197 (2019) 270–276.
[17] J. Peng, Y. Lai, Y. Chen, et al., Small 13 (2017) 1603589.
[18] W. Gu, Y.H. Yan, X.Y. Pei, et al., Sens. Actuators B: Chem. 250 (2017) 601–607.
[19] W. Gu, X. Pei, Y. Cheng, et al., ACS Sens. 2 (2017) 576–582.
[20] Z.Y. Xu, L. Hu, J. Yuan, et al., Adv. Mater. Interfaces 7 (2020) 1902075.
[21] J. Kang, J.D. Wood, S.A. Wells, et al., ACS Nano 9 (2015) 3596–3604.
[22] Z.N. Guo, H. Zhang, S.B. Lu, et al., Adv. Funct. Mater. 25 (2015) 6996–7002.
[23] J.H. Brannon, D. Magde, J. Phys. Chem. 82 (1978) 706–709.
[24] Z. Shen, S. Sun, W. Wang, et al., J. Mater. Chem. A 3 (2015) 3285–3288.
[25] A.G. Kannan, N.R. Choudhury, N.K. Dutta, Org. Lett. 48 (2007) 7078–7086.
[26] J. Wang, R. Sheng, H. Li, et al., Biosens. Bioelectron. 97 (2017) 157–163.
[27] P. Wang, Y. Xia, P.P. Wu, et al., J. Phys. Chem. C 118 (2014) 8891–8898.